SCRIPTA MEDICA (BRNO) – 79 (4): 199–212, *August 2006*

MINERALISATION OF HYALINE CARTILAGE IN THE SMALL-SPOTTED DOGFISH *SCYLIORHINUS CANICULA* L.

EGERBACHER M.[1], HELMREICH M. [1], MAYRHOFER E. [2], BÖCK P. [1]

[1] Department of Pathobiology, Institute of Histology and Embryology,
[2] Clinic of Radiology,University of Veterinary Medicine, Vienna, Austria

Received after revision July 2006

A b s t r a c t

The cartilaginous skeleton of the selachian fish *Scyliorhinus canicula* L. was studied with special emphasis on matrix mineralisation. Calcification of cartilage matrix in selachians neither initiates cartilage destruction nor precedes removal of cartilage, as is the case in mammals. X-ray examination revealed superficially located mineral deposits (cortical calcification, "Rindenverkalkung") in almost all pieces of hyaline cartilage. In vertebrae, additional mineral deposits concentrically embraced the notochord and were seen in lateral segments of the neural arch. Microscopically, hyaline cartilage was inconspicuous besides inorganic deposits in a distinct, 15–45 μm thick band of mineralisation parallel to the cartilage surface. This mineralised area was separated from the perichondrium by an interposed, 20–30 μm thick layer of regularly built cartilage. Calcium carbonate and phosphate were identified histochemically. Organic matrix in mineralised areas showed increased binding of hematoxylin and Periodic acid-Schiff reactivity. Basophilia, metachromasia, and alcianophilia were reduced, and staining with acid fuchsin was prominent. Immunostaining showed significant amounts of keratan sulphate and some collagen type I to substitute for collagen type II. Chondrocytes in mineralised matrix were intact or showed nuclear pyknosis and cellular disintegration. Immunostaining for non-collagenous bone matrix proteins failed in mineralised and non-mineralised cartilage. In the vertebra body, mineral deposits and coarse fibrils of type I collagen were co-localised. Consequently, this tissue was regarded as bony tissue. In lateral segments of the neural arch, such bony tissue was devoid of cells and therefore was identified with bony fish acellular bone. The skeleton of cartilaginous fish offers a model to study mineralisation of cartilage matrix where degenerative or senile changes are excluded. Moreover, calcification of cartilage matrix in shark vertebrae provides an example for studies on direct metaplasia that transforms hyaline cartilage into bony tissue.

K e y w o r d s

Chondrichthyes, Chondrocytes, Calcification, Metaplasia

INTRODUCTION

In adult mammals, matrix calcification in hyaline cartilage is generally assumed to indicate dystrophic changes. Most calcified deposits are situated centrally in larger pieces of cartilage and the frequency of dystrophic calcification correlates with age. In man, regressive changes and mineralisation of hyaline cartilage (thyroid

cartilage, rib cartilage, tracheal cartilage) are well known and accepted as a normal age change, although it may take place as early as at 20 years of age, for instance in the thyroid cartilage, particularly in males (*3, 6, 15, 16*). Calcification may be preceded or accompanied by loss of chondrocytes and severe remodelling of cartilage matrix, giving rise to increased basophilia and occasional appearance of so-called amianthoid fibres (*9*).

During development, matrix calcification occurs in cartilaginous models of bones as a distinct step in the process of secondary ossification. This provisional calcification leads to chondrolysis both in primary ossification centres and in growth plates. The same applies to calcified cartilage in the aged organism, where mineralised matrix is also subject to chondrolysis and precedes ossification (*3, 6*).

The present paper reports on matrix calcification of hyaline cartilage in the elasmobranch fish *Scyliorhinus canicula*, the small-spotted dogfish. Matrix calcification in cartilaginous fish is well known (*2, 8, 11, 12, 13*); it is found as cortical mineralisation next to the cartilage surface, as well as deep in the vertebra body and in the neural arch of vertebrae. It will be described in more detail and discussed with particular emphasis on concomitant changes in organic matrix components, which precede or accompany mineralisation but do not result in chondrolysis and ossification. In this way, calcification of cartilage in chondrichthyes provides a model to study direct metaplasia of chondrocytes, morphologically indicated by remodelling of cartilage matrix and mineral deposition.

MATERIAL AND METHODS

Material: Hyaline cartilage was studied in five specimens of *Scyliorhinus canicula*, kindly provided by the Marine Biology Station Livorno, Italy, and the sea aquarium in Piran, Slovenia. The overall length of the animals was 29–35 cm. The animals were killed by decapitation, roughly reduced to smaller pieces, and fixed by immersion into either 5% neutral formalin (0.2 M phosphate buffer, pH 7.2) or 2.5% phosphate-buffered glutaraldehyde. Before dissection, the specimens were submitted to X-ray analysis. For histological examination, samples were taken from the entire endoskeleton and processed either undecalcified or after decalcification in 4% neutralised EDTA. The specimens were routinely dehydrated and embedded in paraffin. For electron microscopy, small tissue blocks were cut from the gills and fins. The specimens were postfixed in 1% osmium tetroxide (2h at 4 °C), either undecalcified or after decalcification in neutralised EDTA solutions, dehydrated in a series of graded ethanols, and embedded in Epon 812.

Light microscopy: Sections were cut at 5 μm thickness and stained according to the directions in Romeis (*14*):

(1) Hematoxylin & eosin

(2) Van Gieson's method to demonstrate collagen fibres with acid fuchsin

(3) Weigert's resorcin fuchsin for elastic fibres

(4) Binding of colloidal iron hydroxide (Hale's method) for acidic groups

(5) Toluidine blue O staining to demonstrate metachromasia

(6) Alcian blue 8GX at pH 1.0, 2.5, and 4.0 to discern between carboxylic and sulphate groups; the pH 4.0 staining solution was also used after hyaluronidase digestion of the sections (Hyaluronidase type III from sheep testes, Sigma, Munich, D; working solution: 147 U hyaluronidase/ml PBS, pH 6.7) to show the distribution of hyaluronan

(7) Safranin O to show sulphated glycosaminoglycans

(8) Periodic acid-Schiff staining sequence (PAS) for 1´-2´glycolic groups, either without pretreatment or after saliva digestion of the sections

(9) Von Kossa's silver nitrate method to demonstrate calcium deposits, either without pretreatment or after removal of calcium from the sections with 2% acetic acid

(10) Ebel's test to demonstrate phosphates.

Immunohistochemistry: The sections were dewaxed and brought to water. Endogenous peroxidatic activities were blocked with 3% methanolic hydrogen peroxide (20 min, room temperature) and sites of unspecific binding were saturated by pre-incubation in 2% goat serum in PBS for additional 20 min at room temperature. To demonstrate noncollagenous bone matrix proteins, hyaluronidase digestion of the sections was performed as already described (see item 6 in *Light microscopy*). Incubation with the first unlabelled antibody lasted for 1 h at room temperature. The following antibodies from Dakopatts, Glostrup, DK, were used:

(1) Anti-S100 protein (S-100), DK, dilution 1:1,200;

(2) Anti-glial fibrillary acidic protein (GFAP), dilution 1:500;

(3) Anti-vimentin, dilution 1:100;

(4) Anti-smooth muscle α-actin, dilution 1:200.

Antibodies from Chemicon Intern. Inc., Temecula, CA, were:

(5) Anti-bone sialoprotein (BSP), dilution 1:2,000;

(6) Anti-osteonectin (ON), dilution 1:1,500;

(7) Anti-osteopontin (OPN), dilution 1:1,000.

Antibody from Biogenesis, Poole, UK was

(8) Anti-osteocalcin (OC), dilution 1:800.

Antibody from Calbiochem®, San Diego, CA, was:

(9) Anti-keratan sulphate (KS), dilution 1:300

Antibody from Southern Biotechnology, Birmingham, AL, was:

(10) Anti-collagen type I, dilution 1:50, and

Antibody from Quartett, Berlin, D, was:

(11) Anti-collagen type II, dilution 1:50.

Staining for collagens type I and II required digestion of the sections according to the supplier's prescription. To demonstrate collagen type I, sections were digested with 0.1% pepsin in 0.5M acetic acid for 2 h at 37 °C. To show collagen type II, sections were digested with hyaluronidase for 4 h at 37 °C (enzyme solution indicated above), followed by 30 min digestion at 37 °C with 0.1% pepsin in 0.01 N HCl.

After incubation and washing with PBS, antibodies were demonstrated by means of the ABC method (using a standard kit Vectastain® from Vector Laboratories, Burlingame, CA), or by means of the DAKO EnVision™ detection system according to the suppliers' prescriptions. Diaminobenzidine served as a chromogen. Nuclear counterstaining was performed with Mayer's hemalum. Fluorescently labelled secondary antibodies and propidium iodide as a nuclear stain were used to detect anti-collagen antibodies. Fluorescence microscopy was performed with a Leica TCS-NT type laser scanning microscope.

Electron microscopy: Semithin and thin sections were cut on a Reichert OmU3 ultramicrotome. Semithin sections were stained with alkaline toluidine blue O for light microscopy. Thin sections were double-stained with alkaline lead citrate and methanolic uranyl acetate for electron microscopy and viewed with a Zeiss EM 10C electron microscope.

RESULTS

X-ray examination: X-ray examination of our specimens of small-spotted dogfish readily revealed the cartilaginous endoskeleton: The contour of skeletal elements was accentuated by a delicate dense line of constant thickness (*Fig. 1a).* Mineralisation of the vertebrae, by contrast, also affected central areas and was not restricted to a superficial lamina (*Fig. 2a*).

Cortical mineralisation: In tissue sections, a 15 to 45 μm wide band of morphologically altered cartilage matrix was identified equivalent to the dense lines observed in roentgenograms (*Fig. 1b*). This layer of altered matrix was spread out parallel to the cartilage surface, being constantly separated from the perichondrium by a 20 to 30 μm thick layer of non-mineralised cartilage. The external half of this interposed layer of cartilage, just beneath the perichondrium, appeared as subperichondrial cartilage with flattened chondrocytes or chondroblasts; the internal half, next to the mineralised zone, represented inconspicuous hyaline cartilage. Matrix alterations in the mineralised zone concerned increased capacity to bind hematoxylin and multiple spots of unstained crystalline inclusions (*Figs, 1b, 1c*). This layer was entirely blackened with von Kossa's silver nitrate solution (*Fig. 1f*), indicating amorphous calcium deposition in the matrix around the crystals which were blackened as well. The calcified layer fully corresponded to the band of morphologically altered matrix described above, forming a shell that partially or totally separated centre regions from the cartilage surface ("cortical mineralisation" or "Rindenverkalkung"). However, the cartilage inside that shell never showed regressive changes. Intact chondrocytes were also present in mineralised matrix, together with chondrocytes that showed cellular pyknosis and necrosis. Mineral deposits deep to the surface were absent even in larger pieces of cartilage, although selachian cartilage was devoid of vascularisation. There was also no vascular ingrowth to the mineralised cortical layers, which evidently did not impede diffusion of nutrients from the surface to deeper areas.

In cross-sectioned dorsal fins, the cartilaginous rays were seen as a row of oval profiles. Cortical calcification was restricted to the lateral surface of the individual profiles, while cranial and caudal segments in the circumference of the rays remained free of mineral deposits.

Matrix histochemistry: Staining reactions of hyaline cartilage in *Scyliorhinus canicula* did not differ from those in normal mammalian cartilage. The homogeneous, basophilic matrix showed metachromasia with toluidine blue O and bound Hale's colloidal iron preparation, stained with safranin O, showed alcianophilia at pH=4.0 and 2.5, and reduced alcianophilia at pH=1.0 or after hyaluronidase treatment. In the calcified layer, binding of safranin O and alcianophilia were clearly reduced. The mineralised area and the perichondrial layer stained with acid fuchsin when performing van Gieson's method (*Fig. 1d*). When applying the PAS staining procedure, calcified areas reacted stronger than regular cartilage matrix nearby (*Fig. 1e*). All these staining methods left the crystals proper unstained (*Figs. 1b-e*). However, the outline of the crystals was traced by a rim of strongly acidic matrix that deeply stained with safranin O or alcian blue. The von Kossa's method homogeneously blackened the entire calcified layer and crystalline deposits could be discerned no longer (*Fig. 1f*). The same was observed after applying Ebel's test for phosphate.

Immunofluorescence of shark cartilage showed homogeneous distribution of collagen type II except in the calcified areas and in the perichondrial layer (*Fig. 1g*);

both these zones reacted for collagen type I (*Fig. 1h*). Faint but distinct immunoreactivity for keratan sulphate was homogeneously distributed in the matrix but was more pronounced in regions of mineral deposition. Staining for keratan sulphate was also seen in the cytoplasm of chondrocytes irrespective of their location in either unmineralised or mineralised matrix. Chondrocytes reacted for vimentin but did not stain for S-100, GFAP, and smooth muscle α-actin. Immunostaining for non-collagen bone matrix proteins BSP and OC failed. Matrix staining for ON and OPN was absent but faint cytoplasmic staining was noted in all chondrocytes irrespective of their location in either calcified or non-calcified matrix.

Mineralisation of vertebrae: In cross-sectioned vertebrae, areas of mineralisation concerned a) cortical mineralisation that followed the cartilage surface beneath the perichondrium thereby outlining the vertebral body, b) a mighty central ring that closely embraced the notochord, and finally c) lateral segments of the neural arch (*Figs. 2c-e*).

Longitudinal sections of the vertebrae showed the centrally located calcified area as part of two cones which opposed each other with the tips melted together and the bases directed towards the caudal and cranial vertebral surface (*Fig. 2b*). The mineralised ring bordered against the notochord sheath. Here, the matrix was heavily mineralised, whilst the intensity of mineralisation decreased towards the surrounding hyaline cartilage. Mineralised material enclosed flattened to oval chondrocytes in between densely packed collagen fibres (*Fig. 2g*) that stained with acid fuchsin (*Fig. 2e*). A clearly defined boundary was missing where the mineralised cone was contiguous with the surrounding cartilage of the vertebra body. Here, the otherwise compact area of mineralisation continuously disintegrated towards the periphery and multiple small spots of mineralisation were scattered in the cartilage matrix. Chondrocytes within the adjacent cartilage appeared hypertrophic and seemed to form radially arranged serial cartilage (*Fig. 2g*). A narrow calcified band along the surface of the vertebra body represented cortical mineralisation as already described (*Figs. 2c-e*).

Lateral segments of the neural arch were mineralised as well (*Fig. 2c*). These areas were largely devoid of cells, particularly the regions adjacent to the inner aspects of the neural arch. Here, tightly packed coarse bundles of collagen fibres ran parallel to the inner surface, perfectly resembling acellular bone (*Fig. 2d,* arrow in *2f*). These regions deeply stained with acidic fuchsin (*Fig. 1e*) but did not show alcianophilia or affinity for safranin O. Areas of hyaline cartilage were sometimes attached to the outer surface of that acellular bony tissue (*Fig. 2f*). Where the segments of acellular bone ended and hyaline cartilage completed the neural arch, the parallel collagen fibres of acellular bone were seen to continue and to extend into the perichondrial layer of the attached cartilage. This spatial relationship indicates acellular bony tissue as being related to and newly derived from perichondrium rather than to resemble transformation of pre-existing cartilage. At the dorsal end, most chondrocytes achieved hypertrophy and were aligned as serial cartilage along coarse bundles of collagen.

Electron microscopy of cortical mineralisation: Electron microscopy of regularly built cartilage matrix showed extremely delicate collagen fibrils with diameters less than 20 nm and indistinct cross banding periodicity. Any orientation of the fibrils was missing (*Fig. 3a*). Filamentous and granular electron dense precipitates were seen between the fibrils, resembling matrix proteoglycans. Near to the area of cortical mineralisation, these interspersed proteoglycan granules became more numerous (*Fig. 3b*) and additional large electron-dense deposits of irregular shape were noticed (*Fig. 3c*). These deposits were rather homogenous without crystalline substructure, varied in size and showed a tendency to melt together (*Fig. 3d*) and so to obscure any additional morphological detail. Electron dense lines, closely resembling tidemarks of mammalian joint cartilage, were seen within larger deposits. Small foci of electron dense deposits in otherwise normally looking matrix were interpreted as initial deposition of such material (*Fig. 3e*). Initial mineral deposition occurred in cartilage matrix distant to vital chondrocytes and was not necessarily related to cellular debris (*Fig. 3e*), although both intact and necrotic chondrocytes were seen in the mineralised area. Next to the chondrocytes, the delicate collagen fibrils were packed more densely and sometimes orientated in parallel. In rare cases these densely packed fibrils resembled the indistinctly defined large diameter collagen fibrils called "frayed" fibrils.

In the perichondrium, large-diameter collagen fibrils were easily discerned. These fibrils measured up to 100 nm in diameter and formed bundles. Moreover, elastic fibres were also present in the perichondrium.

Technical difficulties prevented electron microscopic analysis of the crystalline deposits seen in the light microscope.

DISCUSSION

The cartilaginous skeleton of sharks, as that of rays and skates, shows a particular form of calcification: Mineral deposits form an inorganic lamella that extends parallel to the cartilage surface. Therefore, the term "Rindenverkalkung" has been chosen in the German literature, indicating the deposition of a crust or rind of mineral (*1*). Although the deposits often extend over wide areas, their thickness remains relatively constant. Smaller deposits are partly separated, partly confluent, forming a mosaic of flattened units (*8; 11*) which show a clear tendency to melt together. The mineralised layer may extend along the entire cartilage surface but more often it remains incomplete. It has been interpreted as mechanical support (*1*) and its distribution on cartilaginous rays in the dorsal fin suggests stiffening against lateral bending as its task. It must be stressed that an interposed layer of regularly built, vital cartilage separates the mineralised zone from the perichondrium. Therefore, the mineralised layer is separated from collagen type I of the perichondrium and nearby connective tissue, as it is separated from the microvascular bed outside the perichondrium.

Mineral deposits in selachian cartilage resemble (at least in part) hydroxyapatite, since this material reduced silver ions, precipitated lead, and was readily removed by diluted acid, indicating the presence of calcium, carbonate, and phosphate ions. This inorganic material was not simply deposed into otherwise unchanged cartilage matrix. In decalcified sections, a severe reorganisation of organic matter became apparent, which evidently had preceded mineral deposition. The total amount of acidic (sulphated) proteoglycans was reduced whilst the concentration of keratan sulphate was increased. Collagen type II was replaced by collagen type I, and as yet undefined homogeneous, PAS-reactive material was deposed. Such reorganisation of cartilage matrix also requires circumscribed decomposition, removal, and degradation of matrix material, a preceding or concomitant cellular task that can be performed by the local chondrocytes only. For these reasons, cortical calcification in selachian cartilage is an index of changes in synthetic activities of the chondrocytes controlling the reorganised area. In fact, these chondrocytes were often found to be vitally looking cells (*8*), and cartilage calcification in selachians is certainly not simply dystrophic, degenerative, or pathological (although necrotic chondrocytes were present as well). Cortical calcification of cartilage in chondrichthyes demonstrates that matrix calcification does not necessarily give rise to degeneration and cell death of chondrocytes in the respective area. Cortical calcification also demonstrates that matrix calcification does not necessarily impede diffusion of nutrients from the surface towards the centre areas, an opinion that is generally hold in histology textbooks (*3, 6*).

Hence, which newly synthesised substance(s) are responsible for mineral deposition? We tested for the presence of non-collagenous, calcium binding bone matrix proteins regularly found in mammalian bone and teeth-bone (BSP, OC, ON, OPN) but none of these could be identified in mineralised or non-mineralised selachian cartilage. Faint cytoplasmic immunostaining for ON and OPN was not restricted to chondrocytes in mineralised areas. Therefore, it seems unlikely that the bone matrix proteins under study initiate mineral deposition in selachian cartilage. Increased concentration of keratan sulphate proteoglycan was noted on the surface of apatite crystals and in the matrix close to the crystals. A comparable situation had been reported by *Nakamura et al.* (*10*), who studied membranous ossification in rat calvaria and found immunoreactivity for keratan sulphate proteoglycan close to calcifying nodules. These authors suggested that proteoglycans might support calcification by trapping calcium ions. The same could apply to calcification of selachian cartilage.

Immunohistochemistry showed collagen type I in areas of mineral deposition where electron microscopy failed to reveal characteristic fibrils. This could indicate impeded fibrillogenesis, probably because of insufficient proteolytic modification of the propeptides. The presence of indistinctly outlined, “frayed” collagen fibrils (*7*) may support this view. As fibrillar type I collagen by itself is not responsible for mineral precipitation (the perichondrial layer remains unmineralised at all), one is tempted to speculate that persisting propeptides could be capable to do so. In

any case, the unknown substance that initiates mineralisation of cartilage matrix is exclusively synthesised by local chondrocytes, as calcium and the anions approach through the perichondrium and calcification does not occur within the layer of intact cartilage that separates perichondrium from the area of calcification. It seems likely that the hypothetical substance represents a glycan or proteoglycan out of the PAS-reactive substances identified in the mineralised areas. Recent studies on dystrophic calcification of the connective tissue of biomaterials (genuine heart valves, heart valve bioprostheses) made clear that mineralisation of these materials also concerns more than simple deposition of inorganic matter into otherwise unchanged matrix. In biomaterials, calcification is preceded or accompanied by deposition of homogeneous sialoglycan material (*5*). Deposition of additional PAS-reactive material also accompanies mineralisation in shark cartilage but in sharks this material is devoid of sialic acid.

Postulation of additional, newly synthesised calcium binding molecules is a common hypothesis to explain regular (developmental) or pathological calcification sites (*4, 5, 10*). However, an alternative hypothesis should be considered as well: It might be assumed that chondrocytes in general synthesise an as yet unidentified substance that prevents mineral deposition in cartilage matrix. If chondrocytes cease to synthesise this substance, matrix calcification will follow. This assumption could explain the proceeding matrix calcification in cell-free areas or in regions with necrotic chondrocytes, where the first hypothesis hardly holds true. Vital chondrocytes in calcified areas are assumed no longer to synthesise the hypothetic substance. In fact, the very same chondrocytes were found to change synthetic activities significantly: The production of a series of cartilage-specific substances (collagen type II, sulphated proteoglycans) was reduced and synthesis of non-characteristic products (collagen type I, additional as yet unidentified glycoproteins) was started. In order to elucidate the mechanism(s) of cartilage calcification, one should search in both directions, for substances apt to initiate calcium precipitation as well as for substances apt to prevent mineral deposition.

Cortical calcification of cartilage in sharks represents direct metaplasia according to Virchow's (*17*) original proposal: Direct metaplasia turns the cells directly into a different mature kind, without cell division but accompanied by necessary modifications to any surrounding matrix. These criteria are fulfilled in the case of cortical calcification, as removal or displacement of cells within hyaline cartilage can be excluded and modification of surrounding matrix is evident. Moreover, the metaplastic tissue is sealed off from the surrounding connective tissue by avascular hyaline cartilage. It is, however, difficult to designate correctly the kind of tissue that is created by the metaplastic changes observed. The terms "mineralised" or "calcified" (hyaline) cartilage have been used throughout this communication while "chondroid bone" might be more appropriate (*2*). The latter term implies an additional step of differentiation towards bony tissue that is already accomplished in the shark vertebrae (*11*). Here, two sites of severe morphological changes should

be discerned: Acellular bone in the neural arch and a particular kind of mineralised tissue (chondroid bone) in the centre of the vertebral body. First, acellular bone in itself is an adverse example to discuss its possible metaplastic origin from a pre-existing different kind of tissue. According to Virchow's (*17*) definition of metaplasia (see above), the phenomenon is initiated by changing metabolic activities of a particular kind of mature cell and these changes are indirectly indicated by the altered surrounding matrix. As acellular bone is free of cells, discussion of its possibly metaplastic origin will fail to yield convincing facts. Considering the texture, nature, and course of collagen fibres within the segments of acellular bone in the neural vertebral arch, together with their obvious continuation into coarse collagen fibres of the connected perichondrium, one is tempted to speculate that acellular bone in sharks directly differentiates from the perichondrial fibrous layer rather than indirectly by metaplasia of hyaline cartilage. Second, mineralised tissue found in the centre of the vertebra body is undoubtedly derived from hyaline cartilage. It enlarges at the expense of the surrounding hyaline cartilage, and closely represents bony tissue in comprising vital cells, mineralised matrix, and mainly coarse fibres of collagen type I (*11*). Enlargement of this bony vertebral centre during growth of the animal undoubtedly requires metaplasia of hyaline cartilage into bone. Disintegration and removal of cartilage matrix make the basis for synthesis and deposition of the new matrix constituents, mainly collagen type I, and deposition of hydroxyapatite crystals. Osteoclasts and osteoblasts or equivalent cells are not involved, as a freely accessible surface is missing. Therefore, one has to conclude that pre-existing chondrocytes are capable of fulfilling the required task and direct metaplasia takes place.

Cartilage of selachian fish provides a useful model to study direct metaplasia of hyaline cartilage into calcified cartilage (cortical mineralisation) and further on (vertebral body) into bony tissue. In mammals, sites with lifelong persisting calcified cartilage comprise the basal layer of articular cartilage, synchondroses, or where the cartilaginous portions of ribs join their osseous segments (*18*). However, where bone is going to substitute for calcified cartilage in mammals, cartilage is destroyed and bone is newly laid down. Direct metaplasia of cartilage or calcified cartilage into bone has not been convincingly demonstrated except where it concerns secondary cartilage, *e.g.* the mandibular symphysis, condyle, coronoid process, angular process, and alveolar processes, the ends of the clavicle, on several bones of the cranial vault, the maxilla and its alveolar processes, the forming penile bone (*2*). Better knowledge of the mechanism(s) which govern and promote the induction of secondary cartilage, cartilage calcification, and finally metaplasia into bony tissue is not only of theoretical interest but could assist modern bioengineering attempts to furnish surgeons with material that will substitute for bone.

A c k n o w l e d g e m e n t

The authors gratefully acknowledge the expert help of PD Dr. Kirsti Witter in preparing the Czech abstract.

Egerbacher M., Helmreich M., Mayerhofer E., Böck P.

MINERALIZACE HYALINNÍ CHRUPAVKY U MÁČKY SKVRNITÉ *SCYLLIORHINUS CANICULA* L.

S o u h r n

Chrupavčitý skelet žraloka *Scyliorhinus canicula* L. byl studován se zvláštním zřetelem na vápenatění mezibuněčné hmoty. Bylo zjištěno, že při kalcifikaci chrupavčité matrix nedochází k odbourávání chrupavky ani jejímu odstranění, jak je pozorováno u savců. Rentgenovým vyšetřením byla prokázána povrchová deposita minerálních látek (kortikální kalcifikace, "Rindenverkalkung") téměř ve všech oddílech chrupavčité kostry žraloka. V obratlech se deposita minerálních solí vyskytovala v koncentrických vrstvách okolo hřbetní struny (notochordu) a v laterálních částech neurálních oblouků obratlů. Mikroskopický obraz byl charakterizován přítomností intaktní hyalinní chrupavky v sousedství deposit anorganických látek, tvořících zřetelný mineralizovaný proužek tloušťky 15-45 μm, uložený paralelně s povrchem chrupavky. Mineralizovaná oblast byla oddělena od perichondria 20-30 μm tlustou vrstvou normální hyalinní chrupavky. Histochemicky byly ve zvápenatělé chrupavce identifikovány uhličitan a fosforečnan vápenatý. Organická matrix mineralizovaných oblastí chrupavky se silně barvila hematoxylinem, vykazovala pozitivní PAS reakci a nižší basofilii, metachromázii a alcianofilii, zatímco kyselým fuchsinem byla zbarvena velmi intenzívně. Imunohistochemicky byl v mineralizovaných okrscích zjištěn ve velkém množství glykosaminoglykan keratansulfát a kolagen typu I, který nahradil kolagen II. Chondrocyty v mineralizované matrix byly intaktní nebo jevily známky pyknózy jader a rozpadu buněk. Přítomnost nekolagenních proteinů nebyla v mineralizované ani nemineralizované chrupavce histochemicky evidována. V tělech obratlů vykazovala deposita minerálních solí kolokalizaci s tlustými vlákny kolagenu I. Tkáň mineralizovaných oblastí chrupavky lze považovat již za kostní tkáň. Ta v laterálních částech neurálních oblouků obratlů neobsahovala vůbec žádné buňky a vykazovala rysy acelulární kostní tkáně popsané u kostnatých ryb. Chrupavčitý skelet žraloků lze využít pro studium procesu mineralizace hyalinní chrupavky, která není ovlivněná degenerativními a senilními změnami, ale i jako model pro studium přímé metaplasie hyalinní chrupavky v kostní tkáň.

REFERENCES

1. *Bargmann W.* Zur Kenntnis der Knorpelarchitekturen (Untersuchungen am Skelettsystem von Selachiern). Z Zellforsch 1939; 29: 405–424.
2. *Beresford WA.* Chondroid bone, secondary cartilage and metaplasia. Baltimore-Munich: Urban & Schwarzenberg, 1981: 325–328, 201–228, 247–260.
3. *Bloom W, Fawcett DW.* A Textbook of Histology. 12th ed. by Fawcett DW, New York: Chapman & Hall 1994: 241–242.
4. *Böck P, Helmreich M, Grabenwöger M.* (2001). Bone matrix proteins are involved in dystrophic calcification of human heart valves. Histochem J 2001; 33: 370–371.
5. *Grabenwöger M, Böck P, Fitzal F, et al.* Acidic glycoproteins accumulate in calcified areas of bioprosthetic tissue. J Heart Valve Disease 1998; 7: 229–234.
6. *Ham AW.* Histology. 6th ed. Philadelphia and Toronto: JB Lippincott Company, 1969: 383–385.
7. *Holbrook KA, Byers PH.* Structural abnormalities in the dermal collagen and elastic connective tissue disorders. J Invest Dermatol 1982; 79: Suppl I, 7s–16s.
8. *Kemp NE, Westrin SK.* Ultrastructure of calcified cartilage in the endoskeletal tesserae of sharks. J Morphol 1979; 160: 75–102.
9. *Mallinger R, Stockinger L.* Amianthoid (asbestoid) transformation: electron microscopical studies on aging human costal cartilage. Am J Anat 1988; 181: 23–32.
10. *Nakamura H, Hirata A, Tsuji T, Yamamoto T.* Immunolocalization of keratan sulfate proteoglycan in rat calvaria. Arch Histol Cytol 2001; 64: 109–118.

11. *Peignoux-Deville J, Lallier F, Vidal B.* Evidence for the presence of osseous tissue in dogfish vertebrae. Cell Tiss Res 1982; 222: 605–614.
12. *Remane A*. Wirbelsäule und ihre Abkömmlinge. In: Bolk L, Göppert E, Kallius E, Lubosch W, eds. Handbuch der vergleichenden Anatomie der Wirbeltiere, Vol IV. Berlin und Wien: Urban & Schwarzenberg, 1936: 1–206.
13. *Remane A, Storch V, Welsch U.* Systematische Zoologie. 5th ed. Stuttgart-New York: Gustav Fischer Verlag, 1997: 551–560.
14. *Romeis B.* Mikroskopische Technik. 17th ed by Böck P, München-Wien: Urban & Schwarzenberg, 1989: 179–249.
15. *Schaffer J.* Lehrbuch der Histologie und Histogenese. 3rd ed, Leipzig: Verlag Wilhelm Engelmann, 1933: 120–132.
16. *Toldt C*. Lehrbuch der Gewebelehre mit vorzugsweiser Berücksichtigung des menschlichen Körpers. 2nd ed, Stuttgart: Verlag von Ferdinand Enke, 1884: 129.
17. *Virchow R.* Das normale Knochenwachstum und die rachitische Störung desselben. Virchow's Arch 1853; 5: 409–507.
18. *Witter K, Egerbacher M, Matulová P, Páral V.* Morphologie der Verbindung zwischen Rippenknochen und Rippenknorpel - eine Diskussion der Begriffe „Synchondrosis" und „Symphysis". Wien Tierärztl Mschr 2004; 91: 214–221.

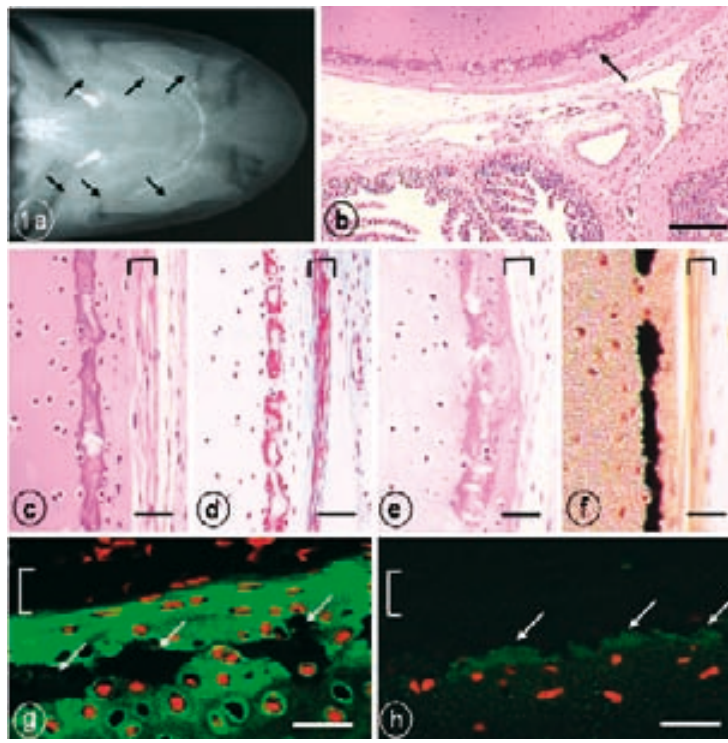

Figs 1a-h
Cortical calcification of cartilage.
1a: X-ray examination of the dogfish head region shows mineralised teeth, ossicles, and vertebrae. The cartilaginous endoskeleton is outlined by delicate dense lines; some of these are indicated by arrows. Natural size
1b: A piece of cartilage beneath the gills shows a continuous line of altered matrix (arrow) that corresponds to the dense outlining observed with X-rays (cf. 1a). Decalcified specimen, H&E staining. Bar = 200µm
1c-f: Staining reactions in areas of cortical calcification. Brackets indicate the perichondrial layer. *1c*: Increased binding of haematoxylin after mineral removal with EDTA. Areas of crystalline deposits are spared out. Note the layer of hyaline cartilage between the region of cortical mineralisation and perichondrial layer (bracket). Decalcified specimen, H&E staining. Bar = 50µm
1d: Acid fuchsin preparations distinctly stain organic matrix in the region of cortical mineralisation and collagen fibres in the perichondrium (bracket). Decalcified specimen, acid fuchsin staining. Bar = 50µm
1e: The PAS staining reveals a higher concentration of 1´-2´glycols in mineralised cartilage matrix. Decalcified specimen, PAS staining. Bar = 50µm
1f: In sections of undecalcified material, von Kossa's silver solution blackens the entire zone of cortical mineralisation. Undecalcified specimen, von Kossa staining. Bar = 50µm
1g: Immunostaining for collagen type II shows normal cartilage matrix as reactive, whilst mineralised areas remain spared out (arrows). The bracket indicates the perichondrial layer. Indirect immunostaining. Bar = 50µm
1h: Immunostaining for collagen type I shows reactivity in mineralised matrix zones (arrows). The perichondrial layer has been lost during preparation; the bracket indicates its position. Indirect immunostaining. Bar = 50µm

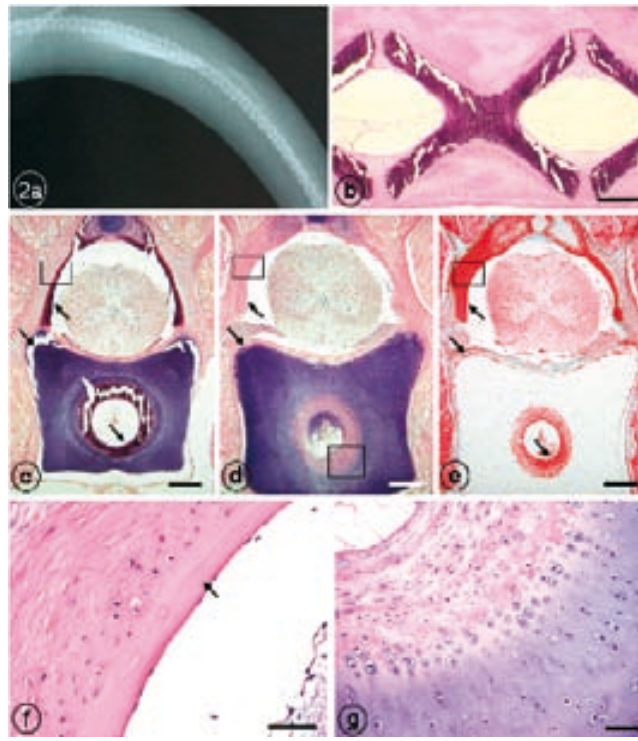

Figs. 2a-g:
Calcification of vertebrae
2a: X-ray photograph showing the dogfish vertebral column. Natural size
2b: Mineral deposits in the vertebra body form pairs of opposing cones with merged apices. Longitudinal section of nondecalcified material, H&E staining. Bar = 200μm
2c-e: Cross sectioned vertebra, showing the distribution of mineral (*2c*), conventional H&E staining after demineralisation (*2d*), and acid fuchsin staining of type I collagen (*2e*) *2c*: Prominent binding of haematoxylin to a mineralised ring embracing the notochord, to areas of cortical mineralisation, and to a mineralised segment of the neural arch (arrows; compare the corresponding boxed regions in *2d* and *2e*). Undecalcified specimen, H&E staining. Bar = 400μm. *2d*: Figure corresponds to *Fig. 2c*. After removal of mineral with EDTA, previously mineralised areas stain eosinophilic (arrows and boxed areas; boxed areas are shown at higher magnification in *Fig. 2f* and *Fig. 2g*). Decalcified specimen, H&E staining. Bar = 400μ. *2e*: Organic matrix in mineralised areas is characterised by coarse bundles of collagen which prominently stain with acid fuchsin (arrows). Cortical mineralisation of the vertebral body now shows up more prominently. Decalcified specimen, acid fuchsin staining. Bar = 400μm
2f: A higher magnification detail of the mineralised segment of the neural arch (upper rectangle in *Fig. 2d*). The arrow points to acellular matrix with prominent lamellar organisation. This tissue component is mineralised (cf. *2c*) and binds acid fuchsin (cf. *2e*). Chondrocytes are restricted to the outer surface of the neural arch. Decalcified specimen, H&E staining. Bar = 100μm
2g: A higher magnification detail of the mineralised ring embracing the notochord (lower rectangle in Fig. *2d*). The mineralised zone is acidophilic, although chondrocytes are present in this area. Note continuous transformation to hyaline cartilage and radially arranged rows of chondrocytes. Decalcified specimen, H&E staining. Bar = 100μm

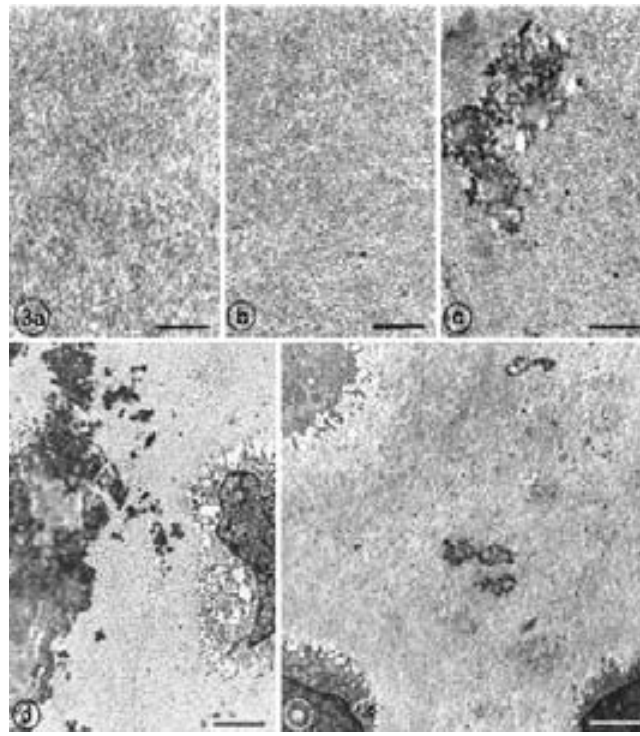

Figs. 3a-e
Electron microscopy of cortical calcification
3a: Electron micrograph shows regular cartilage matrix with irregularly arranged delicate collagen fibrils and a few electron-dense granules. Uranyl acetate and lead citrate staining. Bar = 0.1µm
3b: Next to areas of matrix mineralisation, the amount of electron dense granules increases remarkably. Uranyl acetate and lead citrate staining. Bar = 0.1µm
3c: After decalcification, areas of mineral deposition are readily identified by granules and clusters of electron-dense organic material. This material may obscure possibly present collagen fibrils. Uranyl acetate and lead citrate staining. Bar = 0.1µm
3d: Mineralised matrix in decalcified specimens is characterised by confluent masses of electron-dense material. Note the high number of small electron-dense granules next to the site of calcification and the vitally looking chondrocyte in the right. Uranyl acetate and lead citrate staining. Bar = 2µm
3e: Initial mineral deposition is observed distant to vitally looking chondrocytes; it is not related to cellular necrosis or degeneration. Uranyl acetate and lead citrate staining. Bar = 2µm